Timothy J. Foster
Stephen Ablett
Unilever Research
Colworth House
Sharnbrook
Bedford, MK44 1LQ, UK

Maureen C. McCann
Department of Cell Biology
John Innes Centre
Colney Lane
Norwich, NR4 7UH, UK

Michael J. Gidley*
Unilever Research
Colworth House
Sharnbrook
Bedford, MK44 1LQ, UK

Mobility-Resolved ^{13}C-NMR Spectroscopy of Primary Plant Cell Walls

Primary plant cell walls contain highly hydrated biopolymer networks, whose major chemistry is known but whose relationship to architectural and mechanical properties is poorly understood. Nuclear magnetic resonance spectroscopy has been used to characterize segmental mobilities via relaxation and anisotropy effects in order to add a dynamic element to emerging models for cell wall architecture.

For hydrated onion cell wall material, single pulse excitation revealed galactan (pectin side chains), provided that dipolar decoupling was used, and some of the pectin backbone in the additional presence of magic angle spinning. Cross-polarization excitation revealed the remaining pectin backbones, which exhibited greater mobility (contact time dependence, dipolar dephasing) than the cellulose component, whose noncrystalline and crystalline fractions showed no mobility discrimination. $^1HT_2$ behavior could be quantitatively interpreted in terms of high resolution observabilities. Mobility-resolved spectroscopy of cell walls from tomato fruit, pea stem, and tobacco leaf showed similar general effects.

Nuclear magnetic resonance study of the sequential chemical extraction of onion cell wall material suggests that galactans fill many of the network pores, that extractability of pectins is not dependent on segmental mobility, and that some pectic backbone (and not side chain) is strongly associated with cellulose.

Analysis of the state of cellulose in four hydrated cell walls suggests a noncrystalline content of 60–80% and comparable amounts of $I\alpha$ and $I\beta$ polymorphs in the crystalline fraction. Comparison with micrographs for onion cell walls shows that noncrystalline cellulose does not equate to chains on fibril surfaces, and chemical shifts show that fully solvated cellulose is not a significant component in cell walls. © *1996 John Wiley & Sons, Inc.*

Received July 3, 1995; accepted October 13, 1995.
Biopolymers, Vol. 39, 51–66 (1996)

CCC 0006-3525/96/010051-16

INTRODUCTION

The primary cell wall is an extracellular matrix that is responsible for much of the structural integrity of nonlignified plant tissues. The requirement to accommodate a range of stresses and strains both during active plant growth and in the mature state places significant mechanical demands on the cell wall. These demands are met by a molecular architecture involving polymers (mostly polysaccharides) with varying degrees of self-assembly and interpolymer cross-linking.[1,2] Cellulose arranged in partially crystalline microfibrils is presumed to be responsible for much of the load-bearing ability of the cell wall. One or more of a family of relatively extended polysaccharides conventionally termed hemicelluloses [e.g., xyloglucans and xylans in nongraminaceous species, and β-(1 $\rightarrow$ 3), (1 $\rightarrow$ 4) glucans and (glucurono) arabinoxylans in the *Gramineae*] are thought to be closely associated with cellulose and contribute to intermicrofibril connections. The other major polysaccharide of primary plant cell walls is pectin, which is capable of self-assembly in its carboxylate form in the presence of calcium[3] and may also be covalently linked to other cell wall polymers.[4] Much has been learned of the molecular strength of interpolymer connections by selective and sequential extraction techniques. This approach, for example, has identified a pectic fraction that, together with cellulose, survives 4*M* KOH extraction unlike hemicelluloses that are extracted.[5] Such a pectin–cellulose connection may also be important mechanically. In combination with electron microscopy of cryopreserved cell walls[6] and Fourier transform ir microspectroscopy,[7] chemical/enzyme extractability information has led to the generation of models for primary cell wall architecture[1,2] that can form the basis for further experimentation and refinement.

Nuclear magnetic resonance spectroscopy has been used in a number of ways to probe plant cell walls. Detailed molecular structure and aspects of solution conformation have been studied for e.g. xyloglucan[8,9] and pectin.[10,11] High resolution ^{13}C-nmr spectra of solid cell walls[12,13] and components such as cellulose[14] have been acquired using the techniques of cross-polarization, dipolar decoupling, and magic angle spinning (CP/DD/MAS). This approach allows some resonance assignment, but is most useful in assessing the status of cellulose in cell walls as chemical shifts for C-4 differ significantly between crystalline and noncrystalline states. In addition to frequency-domain spectroscopy, time-domain relaxation approaches have also been used to characterize primary plant cell walls[15,16] and to probe growth[17] and ripening-related[18] changes.

The combination of high resolution separation with appropriate spectral acquisition parameters to discriminate in favor of resonances with particular relaxation characteristics, termed mobility-resolved spectroscopy,[19] provides information on relative mobility/flexibility of molecularly identifiable components within complex systems. This approach has previously been used to study biological macromolecules and assemblies such as deoxyhemoglobin gels,[20] eye proteins,[21] wheat flours,[22] and plant polyesters.[23] In the current study, we have investigated the application of mobility-resolved ^{13}C-nmr spectroscopy to primary plant cell wall material. In all experiments, cell walls were examined directly without changing water content in order to facilitate comparisons with both native tissue and previous electron microscopic studies of hydrated cell wall material.[6] Onion cell wall material has been chosen for most studies as the chemistry is well-defined[5,10] and a scale model for major architectural features has been proposed.[1] A wide range of nmr acquisition parameters have been evaluated in order to provide mobility resolution either by influencing the buildup of magnetization (e.g., single pulse vs cross-polarization) or its decay by relaxation (e.g., dipolar dephasing, variable relaxation delay, variable contact time). Line widths have been influenced via dipole–dipole effects (scalar vs dipolar decoupling) and/or chemical shift anisotropy effects (magic angle spinning).

We have also investigated the effects of sequential chemical extraction on onion cell wall material by mobility-resolved ^{13}C-nmr spectroscopy as well as acquiring spectra for cell walls from different plant sources in order to assess the generality of features observed for onion. The results obtained place limits on current models of cell wall structure and provide dynamic information complementary to microscopic studies. The nmr approaches to mobility-resolved spectroscopy that are evaluated may prove useful in studies of other hydrated biopolymer assemblies.

MATERIALS AND METHODS

Cell wall material was prepared from onion bulbs as described by McCann et al.[6] and sequentially extracted using the method of Redgwell and Selvendran[5] with 50 m*M* CDTA, 50 m*M* Na_2CO_3, 1*M* KOH, and 4*M*

KOH.[6] Tomato pericarp (cv. Ailsa Craig) cell wall material was prepared from red fruit according to Seymour et al.,[24] omitting the dimethyl sulfoxide extraction step. Pea stem cell wall material was prepared from 8 mm stem segments excised from the third internode, 3 mm below the apical hook of etiolated seedlings (*Pisum sativum* var. Arolla) and plunged immediately into liquid nitrogen. Frozen stems were boiled for 10 min in 75% ethanol and then ground to a fine white powder in a mortar and pestle under liquid nitrogen. After further grinding in a glass-on-glass homogenizer on ice, soluble components were removed by centrifugation at 277 K (27,000× *g*, 20 min) and the pellet stored at 193 K. Tobacco leaf cell wall material was obtained by grinding leaves under liquid nitrogen following the procedure described for onion parenchyma.[6] The crude pellet of cell wall material was then washed with 80% ethanol to remove chlorophyll, water washed, and freeze dried. Prior to harvest, plants were grown in the dark for 2 days to minimize starch content.

All cell wall samples were stored frozen prior to examination and were analyzed without removal of water. Dry matter contents were between 3 and 7% w/v and typically ca. 5% w/v. Rapid sample spinning resulted in some compaction of cell wall materials, but recovery of initial hydrated volumes was usually complete after a few hours standing, and repeated acquisition of spectra revealed no significant differences, implying a lack of major structural rearrangement caused by spinning.

Nuclear magnetic resonance spectra were acquired on a Bruker MSL 300 instrument operating at 75.48 MHz for ^{13}C. Sample sizes corresponded to 15–30 mg dry material. Scalar decoupling and dipolar decoupling of 8 and 67 kHz, respectively, were used. Spin-locking fields for cross-polarization/magic angle spinning experiments were ca. 40 kHz. Magic angle spinning speeds were typically 3 kHz and experimental recycle times were 3–5 s. Probe temperatures were 303 K except for frozen samples, which were examined at 233 K. Line broadening of 20 Hz was used for most spectra. Other acquisition parameters and conditions were varied as described below and in following sections.

At the outset of this work, it was anticipated that the highly hydrated nature of the cell wall material used would result in a dispersion of segmental mobilities requiring a range of nmr approaches to characterize polymer chemistries associated with specific motional (correlation time) time scales. In order to characterize the most mobile segments, single pulse excitation was used with either scalar or dipolar decoupling to remove weak and strong dipole interactions, respectively. To test for the presence of chemical shift anisotropy, magic angle spinning was employed. In principle, the combination of dipolar decoupling and magic angle spinning should allow observation of all sites. However, in practice the lengthening ^{13}C T_1 values with increasing segmental rigidity leads to a requirement for very long recycle times to avoid saturation effects. Although recycle times on the minutes time scale may be practicable for bulk high carbon content solids such as coals,[25] for hydrated cell wall material of typically 5% w/v solids, recycle times of 3–5 s were found to be the maximum possible consistent with reasonable signal-to-noise ratios over a total experimental time of 16–18 h. This leads to the nonobservability of signals with ^{13}C T_1 values longer than ca. 5 s, which corresponds to effective correlation times of longer than ca. 100 ns.[26,27] In principle, shorter recycle times can lead to discrimination in favor of more mobile segments with shorter ^{13}C T_1 values. In order to characterize segments with significant segmental rigidity, cross-polarization excitation was used. For cross-polarization to be a useful approach, ^{13}C magnetization must be built up at a rate that exceeds its decay through ^{1}H $T_{1\rho}$ processes. Typical cross-polarization times are ca. 1 ms for protonated carbons, so if ^{1}H $T_{1\rho}$ values are less than ca. 1 ms, then magnetization will not be developed and signal intensity will not be observed. In theory[26,27] this could occur for effective correlation times between 100 ns and 10 μs. In practice, cross-polarization is difficult to establish for short correlation times (<ca. 1 μs) due to motional averaging of the dipolar interactions between ^{1}H and ^{13}C nuclei, and therefore this approach reports on segments with effective correlation times greater than ca. 10 μs. From this analysis, effective correlation times between 100 ns and 10 μs may give severely attenuated signals under both single pulse and cross-polarization excitation. In practice, this has indeed been observed for both a highly viscous solution (lambda carrageenan) and a thin-stranded/segmentally mobile gel (iota carrageenan),[28] and for partly cured epoxy resins.[29] In order to observe all segments in a single experiment, the cell wall samples were frozen (to greatly increase correlation times) and examined by cross-polarization in the frozen state. For those segments that are observable by cross polarization (at ambient temperature), relative mobilities can be probed by, e.g., variation of cross-polarization contact time to discriminate on the basis of ^{1}H $T_{1\rho}$ values, more mobile segments having shorter values, or by dipolar dephasing, which discriminates signals on the basis of the intensity of ^{13}C-^{1}H dipolar interactions. A related approach to defining the range of effective correlation times, but without spectral information, is via the deconvolution of ^{1}H time domain decays into various timescales of ^{1}H T_2 values: an attraction of this approach is that the whole range of segmental mobilities can be observed but the disadvantage is that no structural origins can be derived. The approach adopted in this study was to characterize native onion cell wall material using a range of nmr techniques to establish general features of mobility-resolved spectroscopy, which were then applied to both cell walls from other plant tissues and sequentially extracted onion cell wall material.

RESULTS

^{13}C spectra of onion cell wall material with scalar decoupling and single pulse excitation (i.e., "solu-

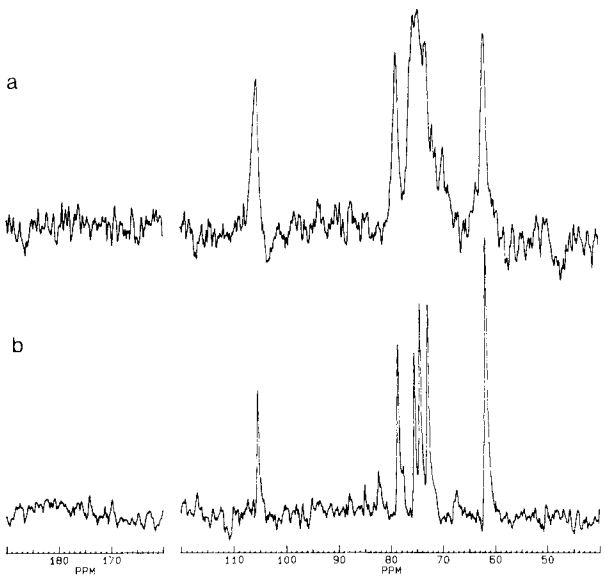

FIGURE 1 Single pulse excitation (SP) ^{13}C-nmr spectra (no line broadening) of (a) onion cell wall material with dipolar decoupling (25,000 scans) and (b) a 5% w/v aqueous solution of lupin galactan.

tion state" conditions) showed insignificant intensity. Under the same acquisition conditions in the presence of dipolar decoupling, a clear spectrum was observed (Figure 1a) with chemical shifts of major signals corresponding to those observed for a solution of lupin (1 → 4)-β-D-galactan (Figure 1b). For the same sample, single pulse excitation with scalar decoupling and magic angle spinning showed a weak spectrum (Figure 2a) with signal chemical shifts consistent with (1 → 4)-β-D-galactan. Much greater intensity was found in the presence of dipolar decoupling (Figure 2b). Galactan signals show slightly greater resolution in the 71–75 ppm region compared to those in the corresponding spectrum in the absence of magic angle spinning (Figure 1a). Additional signals are observed in Figure 2b at 170–180, ca. 100, 68–71 and ca. 54 ppm. These signals have chemical shifts that match those expected[24] for the major pectin backbone of (1 → 4)-α-D-galacturonan with partial methyl esterification: assignments are to C-6 (170–180 ppm); C-1 (100 ppm); C-2, -3, -5 (68–71 ppm); and methyl ester (54 ppm). The C-4 chemical shift is expected at ca. 79 ppm and is possibly seen as a low field shoulder on the C-4 signal for galactan at ca. 78 ppm (Figure 2b). These assignments were validated for onion pectin through the spectrum of an imidazole extract of cell wall material (not shown), which showed two sets of signals corresponding to (1 → 4)-β-D-galactan and (1 → 4)-α-D-galacturonan. Despite the fact that compositional analysis suggests that galacturonan levels are slightly higher than galactan levels,[5] intensity for galactan signals is higher than that for galacturonan signals in Figure 2b, suggesting that some galacturonan is not observable under these acquisition conditions. This is consistent with the observation of galacturonan intensity in the spectrum obtained under cross-polarization, magic angle spinning, and dipolar decoupling conditions (Figure 2c). The major intensity in this spectrum, however, is assigned to (1 → 4)-β-D-glucan (cellulose) with diagnostic signals at 83–85 and 88–89 ppm corresponding to C-4 in "noncrystalline" and "crystalline" cellulose, respectively.[14] This experiment was repeated under frozen conditions, in order to obtain a spectrum (Figure 2d)

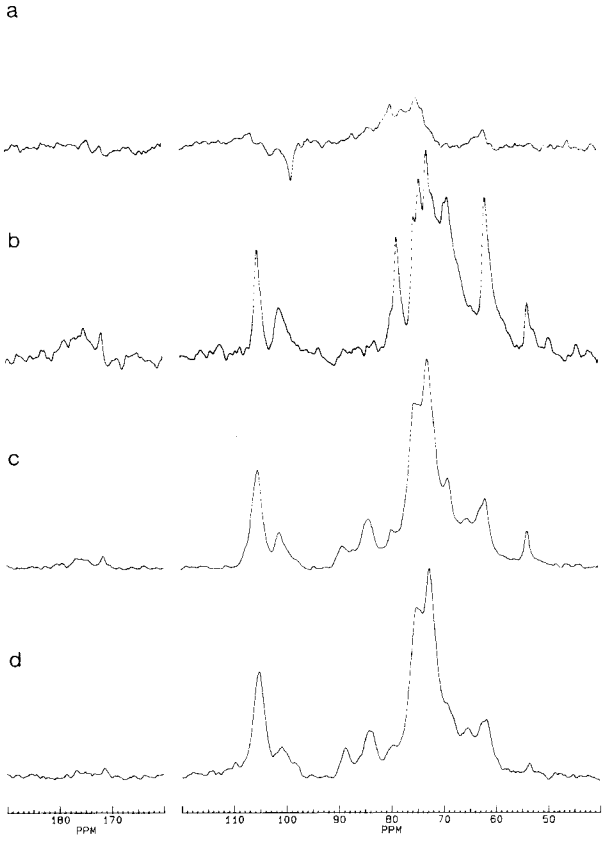

FIGURE 2 Magic angle spinning (MAS) ^{13}C-nmr spectra of onion cell wall material (20 Hz line broadening) (a) with scalar decoupling (SD) and single pulse excitation (20,000 scans), (b) with dipolar decoupling (DD) and single pulse excitation (25,000 scans), (c) with dipolar decoupling and cross- polarization (CP) excitation (1 ms contact time) at 303 K (20,500 scans), and (d) with dipolar decoupling and cross-polarization excitation (1 ms contact time) at 233 K (8,000 scans).

representing all signals for onion cell wall material. This spectrum appears similar to its ambient counterpart (Figure 2c), presumably because polymer segments that are "solid-like" at room temperature will have similar chemical shift dispersions in the frozen state, whereas more mobile segments observed by single pulse excitation at room temperature will give broader resonances in the frozen state due to immobilization of a range of shift-determining conformations.[30] In order to characterize relative carbohydrate segmental mobilities, ^{1}H T_2 behavior was monitored for onion cell wall material that had been extensively washed with D_2O to minimize hydroxyl proton content. The ^{1}H free induction decay comprised three distinct components, the slowest relaxing of which was dominated by magnetic inhomogeneity, and so contained an indeterminate contribution from the residual protons in the D_2O. This part of the time domain signal was further characterized using the Carr Purcell Meiboom Gill pulse sequence into three components,[31] the slowest relaxing of which was assumed to be due to solvent protons. The remaining four components needed to describe the relaxation were quantified as follows: 19 ms (11%), 1.3 ms (14%), 96 μs (14%), and 14 μs (61%). The latter approximates to the rigid lattice limit. From compositional analysis, onion cell walls contain ca. 30% each of galactan, galacturonan, and cellulose with 10% other polymers, particularly hemicelluloses.[5] On the assumption that all galactan is "visible" in a single pulse spectrum with magic angle spinning and dipolar decoupling (Figure 2b), integration gives a galactan to galacturonan ratio of ca. 0.4 and therefore suggests that this spectrum represents ca. 42% (30% from galactan and 12% from galacturonan) of the total cell wall. The cross-polarization spectrum with magic angle spinning and dipolar decoupling (Figure 2c) is assumed to contain all signals from cellulose and hemicellulose. Integral estimates based on C-4 intensity for cellulose and C-1 intensity for galacturonan gives a ratio of ca. 0.5, and therefore suggests that this spectrum represents ca. 55% (30% from cellulose, 10% from hemicellulose, and 15% from galacturonan) of the total cell wall. Comparison of ^{13}C spectral integration with ^{1}H T_2 data suggests that the 14 μs ^{1}H component equates with visibility under cross-polarization conditions, and that other ^{1}H components are equated with single pulse visibility. It would be logical if the 96 μs ^{1}H component was due to the galacturonan backbone and the 19/1.3 ms ^{1}H components were due to galactan side chains.

Within those cell wall segments that are visible

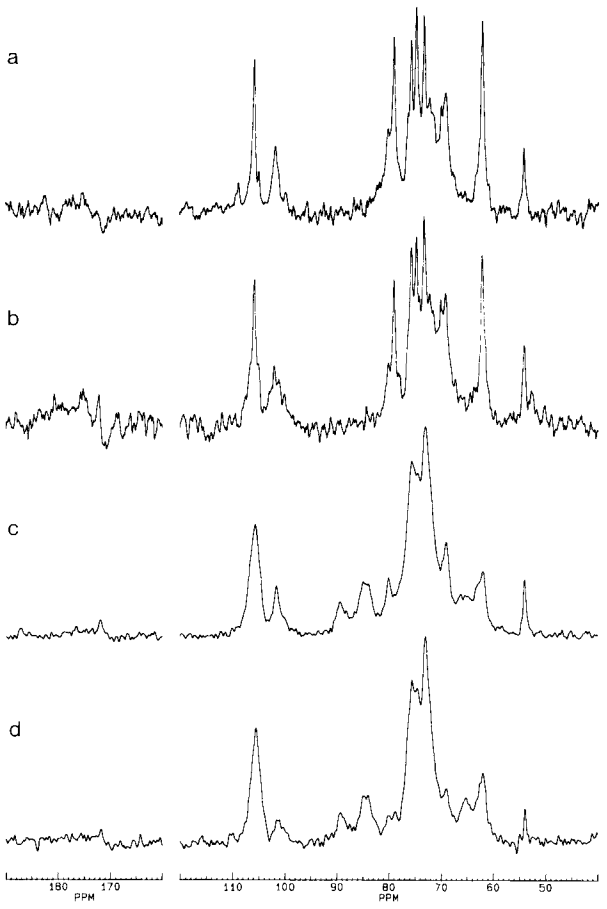

FIGURE 3 ^{13}C-nmr spectra of onion cell wall material: (a) SP/DD/MAS with 0.5 s recycle time (9,000 scans), (b) SP/DD/MAS with 5.0 s recycle time (9,000 scans), (c) CP/DD/MAS with 1 ms contact time (25,000 scans), and (d) CP/DD/MAS with 4 ms contact time (25,000 scans).

under single pulse excitation with dipolar decoupling and magic angle spinning, there may be ^{13}C T_1 variations that could be probed indirectly through changes in spectral repetition rate. Shorter repeat times would be expected to discriminate against sites with longer relaxation times (usually indicative of restricted mobility). However, little difference in absolute or relative intensities is seen between Figures 3a and 3b for recycle times of 0.5 and 5.0 seconds, suggesting that T_1 values for both galactan and visible galacturonan peaks are less than ca. 1 s. Within those cell wall segments with greater rigidity and visible under cross-polarization conditions, variation in intensity with cross-polarization time was monitored as a probe of relative segmental flexibility. Spectra obtained with 1 and 4 ms contact times (Figures 3c and d, respectively) showed a large difference in relative intensity be-

tween signals assigned to cellulose (106, 89, 84 ppm) and galacturonan (100, 79, 54 ppm), with the latter much less intense following the longer contact time. This effect was investigated further by acquiring spectra following contact times of 0.25, 0.50, 0.75, 1.0, 2.5, and 4.0 ms and by monitoring signal intensities. Representative results for two galacturonan and two cellulose signals are shown in Figure 4. For all galacturonan methine and methylene carbons, maximum intensity was at 1.0 ms with a significant reduction in intensity with increasing contact time. For all cellulose carbons, the maximum intensity region was broader, spanning 1.0 to 2.5 ms contact time. There was no detectable difference in intensity variation with contact time between noncrystalline and crystalline cellulose resonances (ca. 83 and 88 ppm, respectively). The different response of signal intensity to contact time for cellulose and galacturonan demonstrates that the two components do not share a common relaxation pathway (^1H $T_{1\rho}$) and is consistent with greater segmental flexibility for galacturonan than cellulose. It is possible that the responses obtained are averages over heterogeneous relaxation environments for each of the polymer types. As a further probe of relative mobilities, dipolar dephasing experiments (in which the ^1H decoupler is turned off for a specified time prior

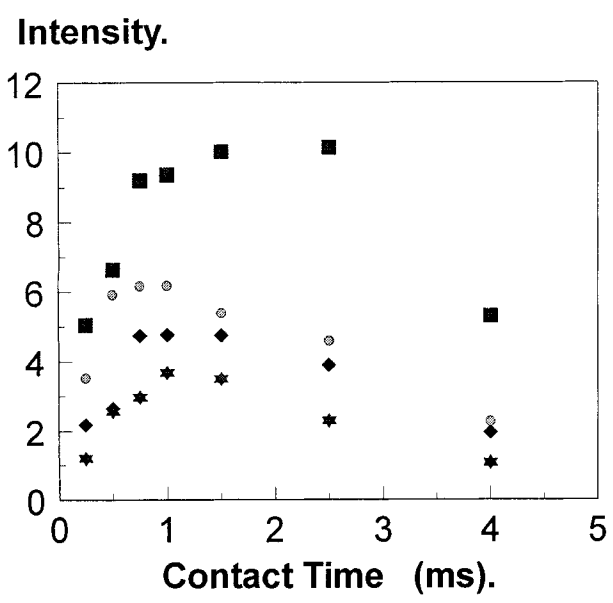

FIGURE 4 Effect of contact time on peak intensity (height) for onion cell wall signals at 106 ppm (■, cellulose C-1), 84 ppm (♦, cellulose C-4 amorphous), 79 ppm (★, pectin C-4) and 69 ppm (●, pectin C-2, -3, or -5) under cross-polarization, magic angle spinning, and dipolar decoupling conditions.

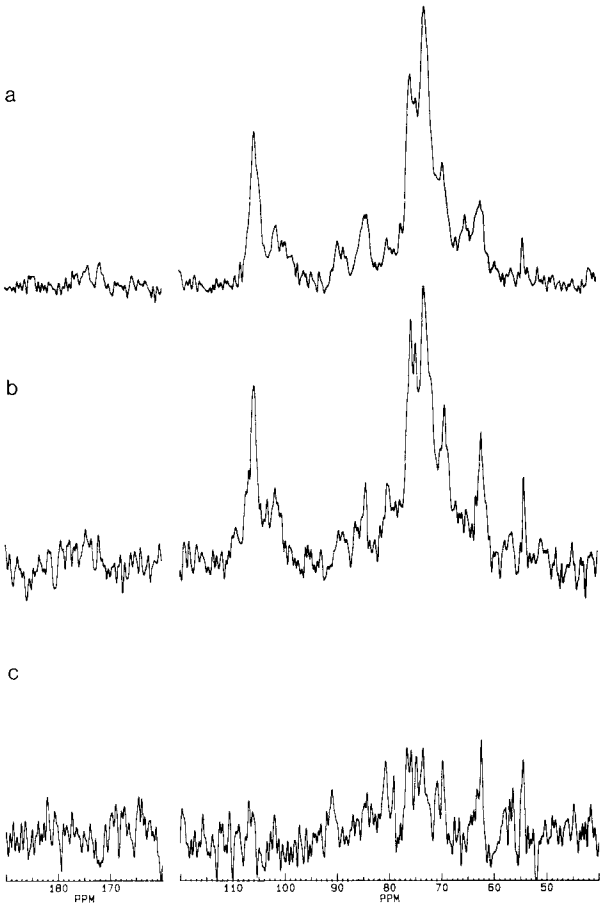

FIGURE 5 ^{13}C CP/DD/MAS spectra (all 25,000 scans) for onion cell wall material with dipolar dephasing times of (a) 10, (b) 25, and (c) 40 μs.

to data acquisition) were carried out. After 40 μs dephasing time, intensity was very weak (Figure 5c) as expected for polymer methylene and methine carbons.[32] For 10 and 25 μs dephasing times, however, significant spectral intensity was observed (Figures 5a and b). Comparison between Figure 5a and Figure 5b suggests that galacturonan signals (most noticeably those at 69 and 79 ppm) are enhanced relative to cellulose signals (e.g., 70–75 and 80–90 ppm) following 25 μs, cf. 10 μs dephasing times. This implies greater internal motions for galacturonan compared with cellulose[33] and provides further evidence for distinct local environments for the two polymer types in the cell wall.

For monitoring the spectroscopic consequences of sequential chemical extraction of onion cell wall material, a common set of nmr experiments were performed. These were single pulse excitation with dipolar decoupling (SP/DD), the same experi-

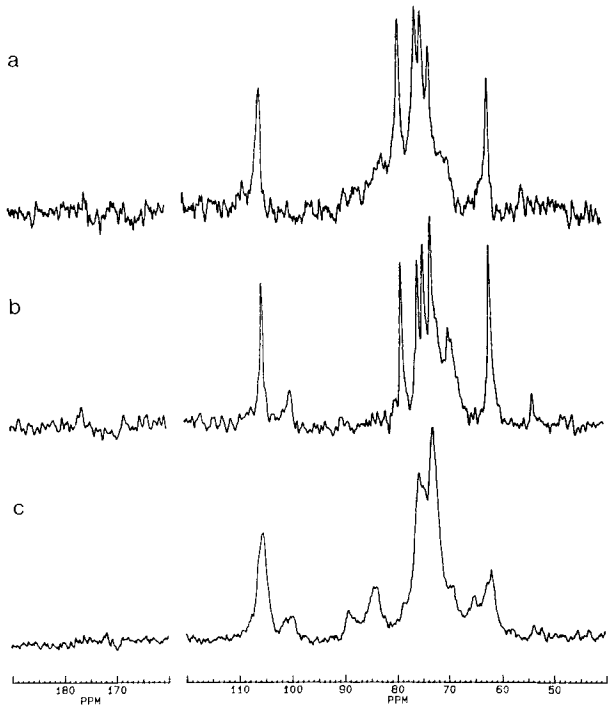

FIGURE 6 ^{13}C-nmr spectra of residual onion cell wall material following extraction with 50 m*M* CDTA (a) under SP/DD conditions at 303 K (25,000 scans), (b) under SP/DD/MAS conditions at 303 K (25,000 scans), and (c) under CP/DD/MAS conditions at 303 K (25,000 scans).

ment in the presence of magic angle spinning (SP/DD/MAS), and cross-polarization excitation with dipolar decoupling and magic angle spinning (CP/DD/MAS). These experiments were carried out at ambient temperature, with the last one also repeated in the frozen state. For onion cell wall material results are shown in Figures 1b, 2b, 2c, and 2d, respectively. Sequential extraction with 50 m*M* CDTA, 50 m*M* Na_2CO_3, 1 *M* KOH, and 4 *M* KOH was carried out[5] with extracted materials characterized in solution by ^{13}C-nmr and residues characterized as described above. CDTA extraction removes a galacturonan-rich fraction with some galactan and results in much sharper galactan features in single pulse spectra (Figures 6a and b) and a decrease in relative galacturonan intensity in both SP/DD/MAS and CP/DD/MAS spectra (Figures 6b and c). Subsequent Na_2CO_3 extraction removes some of the residual galacturonan and more galactan. Residual galactan intensity is enhanced in the SP/DD/MAS experiment compared with the SP/DD experiment (Figure 7a and b), and the only major signals in SP and CP spectra are galactan and cellulose, respectively. Subsequent

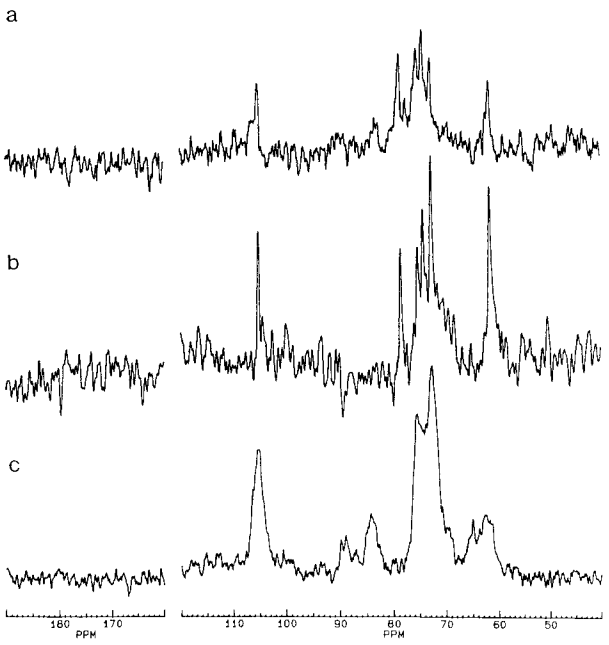

FIGURE 7 As Figure 6 following a subsequent extraction with 50 m*M* Na_2CO_3.

extraction with 1 *M* KOH released mostly galactan together with galacturonan, resulting in a further lowering of galactan intensity (as indicated by decreased signal-to-noise ratio) in the residue observed by SP experiments (Figure 8a and b) and retention of cellulose signals as the dominant fea-

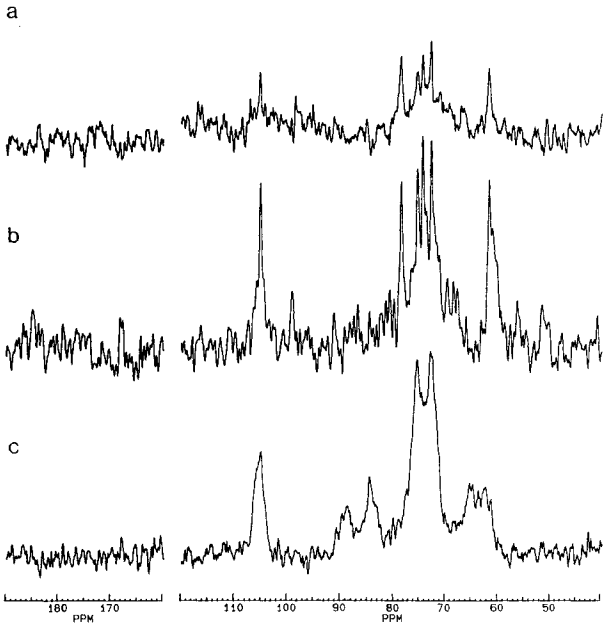

FIGURE 8 As Figures 7 and 6 following a subsequent extraction with 1 *M* KOH.

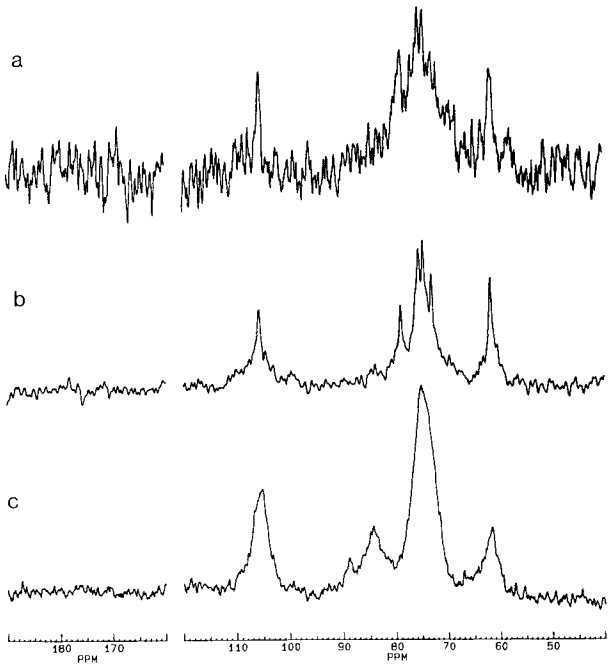

FIGURE 9 As Figures 8, 7, and 6 following a subsequent extraction with 4*M* KOH.

tures in CP experiments (Figure 8c). The final sequential extraction step with 4*M* KOH released a further small amount of galactan and galacturonan. Signals for galacturonan are barely discernable in spectra following Na_2CO_3 or 1*M* KOH extraction steps, yet subsequent extraction steps clearly release galacturonan. This could be due to broad galacturonan signals in the extraction residues because of restricted mobility (single pulse experiments) or conformational diversity (cross-polarization experiments). The 4*M* KOH extraction is the only step that significantly alters the ratio of noncrystalline to crystalline cellulose, as indicated by signals at 83–85 and 88–90 ppm, with an increase in the ratio compared to other cell wall residues (Figure 9c; cf. Figures 2, 6, 7, and 8c). The 4*M* KOH ("α-cellulose") residue contains single-pulse observable galactan and cross-polarization observable cellulose as the main spectral components, although chemical analysis[5] suggests that galacturonan should be present at ca. 60% of the galactan level. Throughout the extraction sequence, CP/DD/MAS spectra at 233 K showed similar signals to those at 303 K (Figures 6–9c) and are not shown.

Figure 10 shows the same set of nmr experiments for (nonextracted) cell wall material from red tomato fruit. Previous compositional analysis[24] suggests 35–40% cellulose, ca. 35% galacturonan, and 5–10% galactan, with a number of other minor components. ^{13}C spectra obtained with cross-polarization (Figure 10c and d) are reminiscent of those for onion cell wall material (Figure 2c and d), with the exception of an increased ratio of noncrystalline to crystalline cellulose. However, the single pulse spectra differ, not only in the expected low level of galactan signals and presence of other (as yet unassigned) signals, but also in the high level of galacturonan features, particularly in SP/DD/MAS spectrum (Figure 10b). Due to the comparable levels of cellulose and galacturonan expected,[24] then, the low galacturonan abundance in Figure 10c is consistent with most of the galacturonan having sufficient segmental mobility to be observable by single pulse techniques.

To explore further the utility of mobility-resolved spectroscopy for the characterization of plant cell walls, material from growing pea stems and tobacco leaves were analyzed by the two "core" experiments of SP/DD/MAS and CP/DD/MAS. For pea stems, the SP/DD/MAS revealed sharp signals not only for (1 → 4)-β-D-galactan but also (1 → 5)-α-L-arabinan[10] at 108.5, 83.3, 81.7, 77.8, and 67.8 ppm (Figure 11a). The

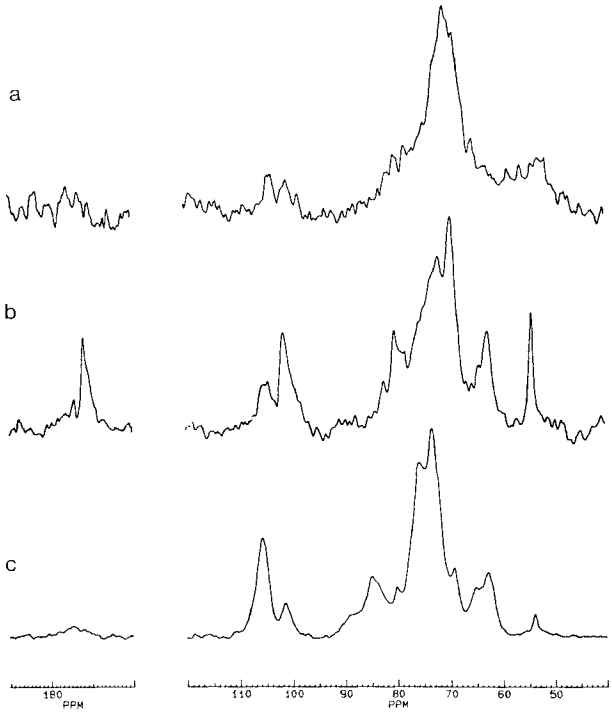

FIGURE 10 ^{13}C-nmr spectra for cell wall material from red tomato pericarp with conditions as for Figures 6–9.

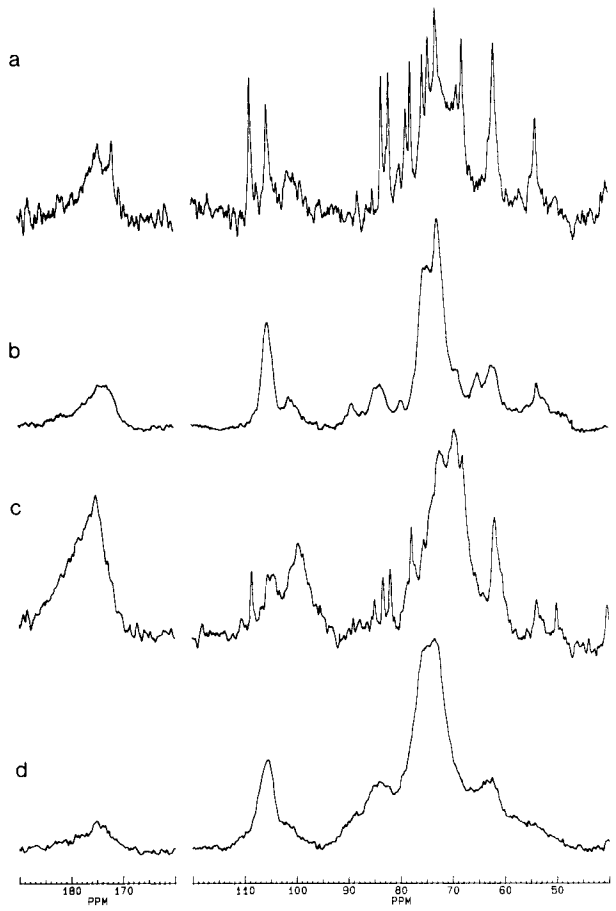

FIGURE 11 ^{13}C-nmr spectra of cell wall materials (a) obtained from ex. pea stem under SP/DD/MAS conditions, (b) ex. pea stem under CP/DD/MAS conditions, (c) ex. tobacco leaf under SP/DD/MAS conditions, and (d) ex. tobacco leaf under CP/DD/MAS conditions.

relatively intense signal for the methyl ester substituent of galacturonan (54 ppm) suggests that the broad signal around 100 ppm is due to the C-1 resonance of galacturonan in either a range of shift-determining environments or with a residual broad line. The presence of a substantial arabinan component is consistent with chemical analysis.[34] As for other systems, the pea stem cell wall CP/DD/MAS (Figure 11b) response is dominated by cellulose with some galacturonan. For tobacco leaf cell walls, the SP/DD/MAS spectrum contains major features for galacturonan (broad) and arabinan (sharp), with other intensities possibly due to relatively broad galactan signals (Figure 11c). The high intensity at 170–180 ppm is assigned to protein in addition to galacturonan. The corresponding CP/DD/MAS spectrum (Figure 11d) is broad and dominated by cellulose with some galacturonan.

DISCUSSION

Mobility-Resolved Spectroscopy of Hydrated Cell Walls: Methods and Limitations

The natural hydrated state of primary plant cell walls in vivo makes the study of structural and motional properties of isolated cell wall material more relevant in a hydrated environment. Previous nmr studies of plant cell walls have focused on spectroscopy of low moisture systems[12,13] or relaxation behavior in hydrated systems with no spectral information.[15–17] The inherent problem associated with highly hydrated primary cell wall samples (typically 5% w/v dry matter) for ^{13}C-nmr is one of signal-to-noise exacerbated by often broad lines and only partial visibility in any one experiment. The benefits are that spectral "fingerprints" for major polymer components are known and can hence be recognized in spectra obtained under conditions favoring defined segmental flexibilities. From the present study it seems probable that only quantitatively major components (>10% of total) are reliably observed for total experimental times up to 16 h. For example, signals for rhamnose, an important component in the backbone of pectins,[35] are not unambiguously observed as the total abundance (in onion cell walls) is less than 2%.[5] A second general conclusion is that hydrated primary plant cell walls exhibit a very broad range of segmental flexibilities and that some components (cellulose, galactan) have characteristic flexibilities whereas others (galacturonans) exhibit a broad range of segmental flexibility. This behavior is in contrast to the polysaccharide-based cell walls of yeast, which appear to be fully observable under SP/DD/MAS conditions in the hydrated state.[36] It is possible that the greater permanence and the various demands of a multicellular tissue on constituent cell walls has resulted in the adoption of a motionally heterogeneous network in plants.

Within the broad classes of single pulse and cross-polarization spectroscopy, a number of mobility-resolving approaches were found to be useful. For single pulse excitation, the strength of proton decoupling required for signal visibility (dipolar, not scalar) indicates the presence of strong dipolar interactions for galactan and other side chains. Additional magic angle spinning may

average some residual dipolar coupling under scalar decoupling conditions, but the primary effect is expected to be removal of line broadening contributions resulting from chemical shift anisotropy. In all cases this distinguished side-chain galactan (SP/DD visible) from some backbone galacturonan (SP/DD invisible but SP/DD/MAS visible). It might have been anticipated that relatively short correlation times (10^{-7}-10^{-8} s) would lead to T_1 values on the seconds time scale,[27] but varying recycle times between 0.5 and 5.0 s did not cause significant spectral changes, thus making this approach to mobility-resolution inappropriate for onion cell wall material.

For cross-polarization excitation, mobility resolution can be achieved through variation in cross-polarization rates and ^1H $T_{1\rho}$ values for different sites, by dipolar dephasing to probe the motionally induced dissipation of magnetization, or potentially via ^{13}C T_1, measurements. The first two can be probed in variable contact time experiments in which intensity for each site rises at the cross-polarization rate and decays under the influence of the associated ^1H $T_{1\rho}$. Spectra obtained at 1 and 4 ms contact times show major differences in relative intensity between galacturonan and cellulose resonances (Figure 3c and d) in onion cell walls. Signal intensities as a function of contact time (Figure 4) suggest that the origin for this difference lies in a more rapid loss of intensity for galacturonan signals (maximum intensity at 0.75–1.0 ms) than for cellulose signals (maximum intensity 1.0–2.5 ms). No attempt has been made to quantify build up or relaxation rates due to the relatively low signal-to-noise ratio. It is also quite possible that unique values cannot be associated with each polymer type. In particular, given the motional heterogeneity of galacturonans, it might be expected that a range of ^1H $T_{1\rho}$ values may be associated with this component.

A further demonstration of the overall greater relative segmental mobility of galacturonan compared with cellulose is shown by dipolar dephasing experiments (Figure 5). This experiment is normally used to distinguish CH and CH_2 groups from CH_3 and quaternary carbons as the latter two lose less intensity than the former two during a dephasing delay because greater mobility (CH_3) or lack of attached protons reduces the strength of ^{13}C-^1H dipolar interactions.[37] For synthetic polymers, this approach has been used recently to distinguish between backbone and side-chain CH and CH_2 sites in bulk and resin[33] states. Figure 5c shows the essentially complete loss of signal after 40 μs, consistent with previous reports for proteins.[32] Relative intensities following 10 and 25 μs dephasing times (Figure 5a and b) suggest a more rapid loss of cellulose intensity than galacturonan intensity, which is attributed to greater segmental mobility in the latter. The complementary techniques of variable contact time and dipolar dephasing[37] probe mobility variation on the 10^{-4}–10^{-6} s time scale. Relaxation effects on a longer time scale might be detectable from ^{13}C T_1 measurements, as data for bulk cellulose[38] yielded values between 4 and 130 s. Discrimination between resonances on the basis of ^{13}C T_1 can be achieved by a delay following cross-polarization in which both ^{13}C and ^1H power is off, followed by an observation (90°) pulse in the presence of dipolar ^1H decoupling.[39] The problem with this approach for motionally heterogeneous systems is that the observation pulse corresponds to the SP/DD/MAS experiment and hence composite spectra of attenuated CP and full SP intensities are observed. This effect was indeed observed with differing spectra observed following, e.g., 10, 20, or 40 s delay (data not shown), but interpretation was compounded by difficulties in phasing spectra with combined SP and CP observable signals. Although several approaches to achieving mobility resolution have been successful, they often give the same general information. The primary distinction is between single pulse and cross polarization excitation. Within the SP "family" both ^1H decoupler power and MAS variation gave useful information. Within the CP "family," the variable contact time experiment is the most helpful for hydrated cell walls.

A Common Motional Hierarchy in Hydrated Primary Cell Walls

Motional heterogeneity in hydrated bean cell walls has previously been deduced from ^1H relaxation measurements.[15] T_2 values of 30 and 80 μs were assigned to polymer segments, with values of 4.5 ms up to 1 s assigned to water protons. The 30 μs component was assigned to cellulose and hemicelluloses, and the 80 μs component was assigned to pectin and hemicellulose with the relative intensity of components being 80:20, respectively.[15] For onion cell walls, the major T_2 component (61% of intensity) was close to the rigid lattice limit and is assigned to cellulose, hemicellulose, and some galacturonan, and probably corresponds closely to signals observable in a CP/DD/MAS experiment. A T_2 component (14% of intensity) of ca. 100 μs is assigned to the remainder of the galacturonan,

requiring DD and MAS conditions for observation by single pulse excitation. The two longest polymer-attributed T_2 components of 1.3 ms (14% intensity) and 19 ms (11% intensity) are assigned to galactan. It has been found previously that two exponential components are required to describe the time domain signal from flexible polysaccharides.[31] ^{1}H T_2 behavior therefore can be closely linked to spectral observability with the added benefit of relative quantitation of relaxation contributions that can be linked directly to chemical analysis.

Results for red tomato pericarp (dicotyledonous parenchyma), pea stem, and tobacco leaves have certain features in common with onion bulb (monocotyledonous parenchyma) cell walls. In all ambient CP/DD/MAS spectra (Figures 10c, 11b, and 11d), cellulose is predominant, with signals characteristic for galacturonan (170–180, ca. 100, ca. 79, ca. 69, and ca. 54 ppm) clearly visible in tomato and pea stem spectra and probably present in tobacco leaf. It might be expected that hemicellulose signals would be observed in CP/DD/MAS spectra. However, some expected signals (e.g., 1 → 4-β-linked glucose in xyloglucan and glucomannan) might be coincident with cellulose signals, whereas other C-1 sites would be close to cellulose (mannose in glucomannan, galactose in xyloglucan) or galacturonan (xylose in xyloglucan) signals.[40,41] Information on cellulose/hemicellulose interactions and networks could only be obtained reliably in the absence of pectic material. In common with onion, cell wall material from tomato pericarp, pea stem, and tobacco leaves have SP/DD/MAS spectra that lack cellulose and contain signals for galacturonan and pectic side chains. For pea stem (Figure 11a) sharp signals are observed corresponding to both (1 → 4)-β-D-galactan and (1 → 5)-α-L-arabinan. For tobacco leaf (Figure 11c) sharp signals correspond to (1 → 5)-α-L-arabinan, whereas a broad signal at the C-1 shift for (1 → 4)-β-D-galactan (105 ppm) suggests either structural heterogeneity (e.g., branching) or the presence of a different polymer (e.g., xylogucan and/or glucomannan) with a similar C-1 shift. For tomato (Figure 10a and b) it is known that galactan is relatively sparse in the red fruit[24]; as for tobacco leaf, broad C-1 spectral features (ca. 105 ppm) suggest either structural heterogeneity or overlapping resonances from another polymer. For both pea stem and particularly tobacco leaf, high intensity in the carbonyl region (170–180 ppm) coupled with intensity in the 20–40 (aliphatic) and 120–130 (aromatic) ppm regions are diagnostic of proteins. Protein resonances differed significantly between SP/DD/MAS and CP/DD/MAS spectra in both cases, indicative of motional heterogeneity in proteins as well as polysaccharides in cell wall material. Taken together, these results illustrate a common motional hierarchy in hydrated primary plant cell walls with pectic side chains more mobile than a fraction of the pectin backbone. Other pectin backbone regions show less mobility, but are not as rigid as cellulose.

Sequential Chemical Extraction of Onion Cell Wall Material: Pectin Extractability Is Not Associated with Segmental Mobility

Much information about the relative strength of attachment of polymers to cell wall matrices can be obtained by sequential chemical extraction methods designed to remove classes of polymers attached in defined ways while minimizing effects on other polymers. One such approach was developed in studies of onion cell walls[5] and has been adopted in this study, allowing comparison of results not only with chemical analysis[5,10] but also direct microscopic visualisation.[6] One immediate comparison can be drawn with respect to the galactan component, which is known to be present as relatively short (average ca. 8 galactose units) side chains of pectin with narrow lines in solution ^{13}C-nmr (SP with scalar decoupling).[10] The lack of observability of galactan side chains in microscopic images[6] may be due to folding back onto backbones. The requirement for dipolar decoupling for observation of cell wall galactan signals in single pulse experiments indicates stronger dipolar coupling in cell wall (cf. solution) environments, presumably reflecting motional inhibition. This comparison suggests that galactan may be significantly entangled in the cell wall matrix with the implication that many of the apparent pores observed microscopically[6] may be significantly occupied by galactan side chains in the hydrated state. Pore sizes of 10 nm or less were estimated by microscopy[6] but these correspond only to framework polymers not side chains. (1 → 4)-β-D-galactan is suggested to have a twisted chain configuration with pseudo-helical elements[42] leading to an estimate of ca 0.3 nm per galactose residue in projection. For average onion galactan lengths this corresponds to 2–3 nm per side chain. Given the large galactan content, several side chains may be present in each "pore" leading to an effective space filling.

The first stage of the sequential extraction process involves removal of a significant fraction of galacturonan with some galactan by the action of the

calcium-chelating agent CDTA,[5] although it is not clear whether calcium chelation is the critical factor.[43] The nmr spectra show depletion of galacturonan relative to both galactan in SP/DD/MAS spectra (Figure 6b; cf. Figure 2b) and cellulose (Figure 6c; cf. Figure 2c) in CP/DD/MAS spectra in approximately equal amounts. This indicates either that two separate galacturonan-rich polymer families (differing in segmental flexibility in the cell wall) are extracted, or that individual galacturonans contain segments differing in wall mobility. In the absence of any mechanism or supporting evidence for the former, we favor the latter explanation, particularly as the polymers extracted are found to be much longer than the diameters of network pores.[6] Sharper galactan signals in the SP/DD experiment after CDTA extraction (Figure 6a; cf. Figure 1a) are taken as evidence that the galacturonans extracted with CDTA serve to constrain the segmental motion of galactans within the wall. Sodium carbonate extracts most remaining galacturonan with associated galactan (and less abundant arabinan) side chains.[5,10] This is manifested in loss of galacturonan signals in both SP/DD/MAS (Figure 7b) and CP/DD/MAS (Figure 7c) spectra. Residual spectra are dominated by galactan (SP/DD/MAS) and cellulose (CP/DD/MAS). Subsequent 1 *M* KOH extraction removes primarily a galactan-rich polymer, again resulting in SP/DD/MAS (Figure 8b) and CP/DD/MAS (Figure 8c) spectra dominated by galactan and cellulose features. Further extraction with 4 *M* KOH removes a fraction corresponding in composition to xyloglucan.[5] Diagnostic C-1 signals for xyloglucan at ca. 105, 103, and 100 ppm[40] were observed in nmr spectra of the 4 *M* KOH extract (data not shown), so evidence for signals in the 1 *M* KOH residue spectra was sought. It is possible that a very weak signal at ca. 100 ppm in SP/DD/MAS spectra of both Na_2CO_3 and 1 *M* KOH residues (Figures 7b and 8b) is due to xylose C-1 sites in xyloglucan. Galactose C-1 in xyloglucan has a very similar chemical shift to both galactan and cellulose, and so is unlikely to be observed. Glucose C-1 in xyloglucan (expected at 103.4 ppm[40]) may be the origin of a very weak signal in this region in the Na_2CO_3 extract (Figure 7b), but assignments cannot be made with certainty. The expected abundance of xyloglucan (10% of total cell wall polysaccharides, but 20% in the 1 *M* KOH residue) would suggest that signals should be detectable, but overlap with other signals and probable motional heterogeneity preclude further investigation of the proposed cellulose/xyloglucan network[6] in hydrated onion cell walls. The 4 *M* KOH (α-cellulose) residue corresponds to ca. 45% of the total cell wall material and contains ca. 60% cellulose, 20% galactose, and 12% galacturonan.[5] Figure 9 shows that remaining galactan retains sufficient segmental flexibility for visibility in a SP/DD/MAS experiment (Figure 9b), although magic angle spinning (cf. Figure 9a) is needed for high signal intensity. This is interpreted as being due to the collapsed[6] cellulosic framework causing additional chemical shift anisotropy to be experienced by galactan side chains that otherwise retain segmental flexibility. Galactans are attached to galacturonan polymers at C-4 of backbone rhamnose residues.[35] The segmental flexibility evident for galactan in the 4 *M* KOH residue suggests that attachment to the residual cell wall framework is via (rhamno)galacturonan sequences, presumably directly associated with cellulose. This attachment is strong enough to withstand apparent microfibril expansion[6] and the partial conversion of crystalline to noncrystalline cellulose, as evidenced by relative intensities for C-4 signals at ca. 88 and 83 ppm, respectively. Approximate estimates of crystalline: noncrystalline ratios before and after 4 *M* KOH extraction (Figures 8c and 9c) are 60:40 and 80:20, respectively. A similar effect was noted in a study by CP/DD/MAS nmr of the sequential extraction of *Vigna radiata* cell walls.[12]

The study of sequential cell wall extraction by mobility-resolved nmr has enabled a number of conclusions to be drawn concerning abundant polymers within onion cell walls. In particular, galactan side chains probably act as effective pore fillers, extractability of pectins is not dependent on segmental mobility, and pectic material that resists 4 *M* KOH is more likely to be associated with cellulose via backbone rather than side-chain regions. The main drawback is that the low signal-to-noise for such highly hydrated and motionally heterogeneous networks precludes the study of components present at 10% or less of the cell wall. Information obtained, however, complements that from high resolution microscopy,[6] chemical analysis,[5] and other modern methods of cell wall analysis.[44]

On the State of Cellulose in Primary Cell Walls

High resolution ^{13}C-nmr (particularly the CP/DD/MAS experiment) has provided much information on the extent of molecular ordering and the nature of crystalline cellulose polymorphs[14,45,46] and relaxation characteristics for bulk celluloses.[38]

Recent studies on partially hydrated cell walls have reported on the level of crystalline order[13] and details of polymorphic form and noncrystalline order.[47]

Crystalline and noncrystalline (often referred to as "amorphous") sites within cellulose are most obvious for C-4 resonances centred at 88–90 and 83–85 ppm, respectively.[14] In the highly hydrated cell wall materials used in the present study, relative integrals for C-4 peaks in ambient CP/DD/MAS spectra (Figures 2c, 10c, 11b, and 11d) suggest crystalline to noncrystalline ratios of ca 40:60 (onion), 20:80 (tomato), 35:65 (pea stem), and 25:75 (tobacco leaf). The relevant figure for apple cell walls has been quoted as 38:62.[14] The explanation for this latter ratio was based on the suggestion that the crystalline resonance corresponds to sites in the interior of microfibrils with the non-crystalline resonance due to surface sites. In order for the observed ratio to be explicable, it was suggested that average microfibril cross-sections were 3.0 × 2.7 nm.[14] Whereas there are no reports of accurate microfibril dimensions in apple, the onion cell walls used in the current study have an average cellulose fibril diameter of 8 nm[6] requiring average cross sections of the order 6 × 6nm. This leads to a ratio of internal to surface chains of 64:36 in contrast to the C-4 intensity ratio of 40:60 crystalline to noncrystalline. We conclude that for onion cell wall, surface chains alone are not sufficient to account for the noncrystalline resonance. This is in line with previous results for bulk cellulose nmr[38] and cellulase action patterns,[48] which suggest "amorphous" zones within cellulose microfibrils. As onion cell walls had the highest crystalline C-4 content of those studied, it is reasonable to assume that the signal at 83–85 ppm is in general not due entirely to surface chains and that there must be regions within cellulose chains that are less ordered than others. In contrast, cellulose produced by *Acetobacter xylinum* has a crystalline content of up to 80–85%,[45] but exists as a thin ribbon with a corresponding high level of surface chains. For this system the implication is that surface chains could in nmr terms be classified as crystalline. The same argument also applies to assignment of intensity at 83–85 ppm to surfaces of crystallites within chains. An even more extreme example is *Valonia* cellulose, which has virtually no noncrystalline resonances.[45,46] Evidence for significant molecular order in noncrystalline cellulose is obtained by comparison with chemical shifts for oligomeric celluloses in aqueous solution.[49] C-4 shifts (taking account of the different referencing system used by Heyraud et al.[49]) for solutions of the disaccharide to hexasaccharide are ca. 80 ppm, i.e., 3–6 ppm upfield from the signal for noncrystalline cellulose. The absence of significant intensity for celluloses in hydrated environments at the chemical shift characteristic for oligomers in aqueous solution suggests that an insignificant fraction of cell wall cellulose is present as fully solvated chains, and that the signal at 82–86 ppm should be regarded as being due to a molecularly organized form of cellulose.

In support of this assignment, resolution enhancement of C-4 signals (Figure 12) suggests that defined chemical shifts of ca. 83.5 and 85.0 ppm are important contributors to intensity of the 82–86 ppm signal, as first illustrated by Newman et al.[47] for apple cell walls and microcrystalline cellulose. This was interpreted[47] as evidence for distinct crystallographically inequivalent sites on the surface of highly crystalline microfibrils. In the light of the above discussion, we assign these resonances resolved by resolution enhancement to have specific molecular order characteristics (e.g., hydrogen-bonding arrangements or chain alignment) without full crystalline order, but not to be uniquely associated with either surface or interior chains.

^{13}C-nmr can be used to estimate the relative abundances of Iα and Iβ crystal forms. Characteristic signals at 104.3 and 106.3 ppm (C-1), and 88.2 and 89.2 ppm (C-4) due to the monoclinic Iβ form[14,45,46] are all at least partially resolved for onion and tomato cell walls (Figure 12). The triclinic Iα form contributes signals at 89.2 and 90.2 ppm (C-4) and 105.5 ppm (C-1). Due to the coincidence of crystalline and noncrystalline C-1 signals, only C-4 signals can be used to assess the relative abundance of the Iα and Iβ forms. Comparison with C-4 line shapes for quantitatively analyzed cellulose spectra[45,46] suggests that tomato, onion, and pea stem cell walls contain comparable (40/60 to 60/40) amounts of the two crystal forms, consistent with results for apple cell walls and suggesting that this may be a general feature of primary cell walls.

It is interesting that cross-polarization dynamics (both build up and decay) were insignificantly different for crystalline and noncrystalline cellulose C-4 signals as indicated by the same relative intensity as a function of contact time (e.g., Figure 3c,d). This implies that dipolar coupling and (lack of) segmental motion on the μs time scale are very similar for sites contributing to the two signals, and is consistent with the results of Newman et al.,[47] who were unable to generate subspectra on the ba-

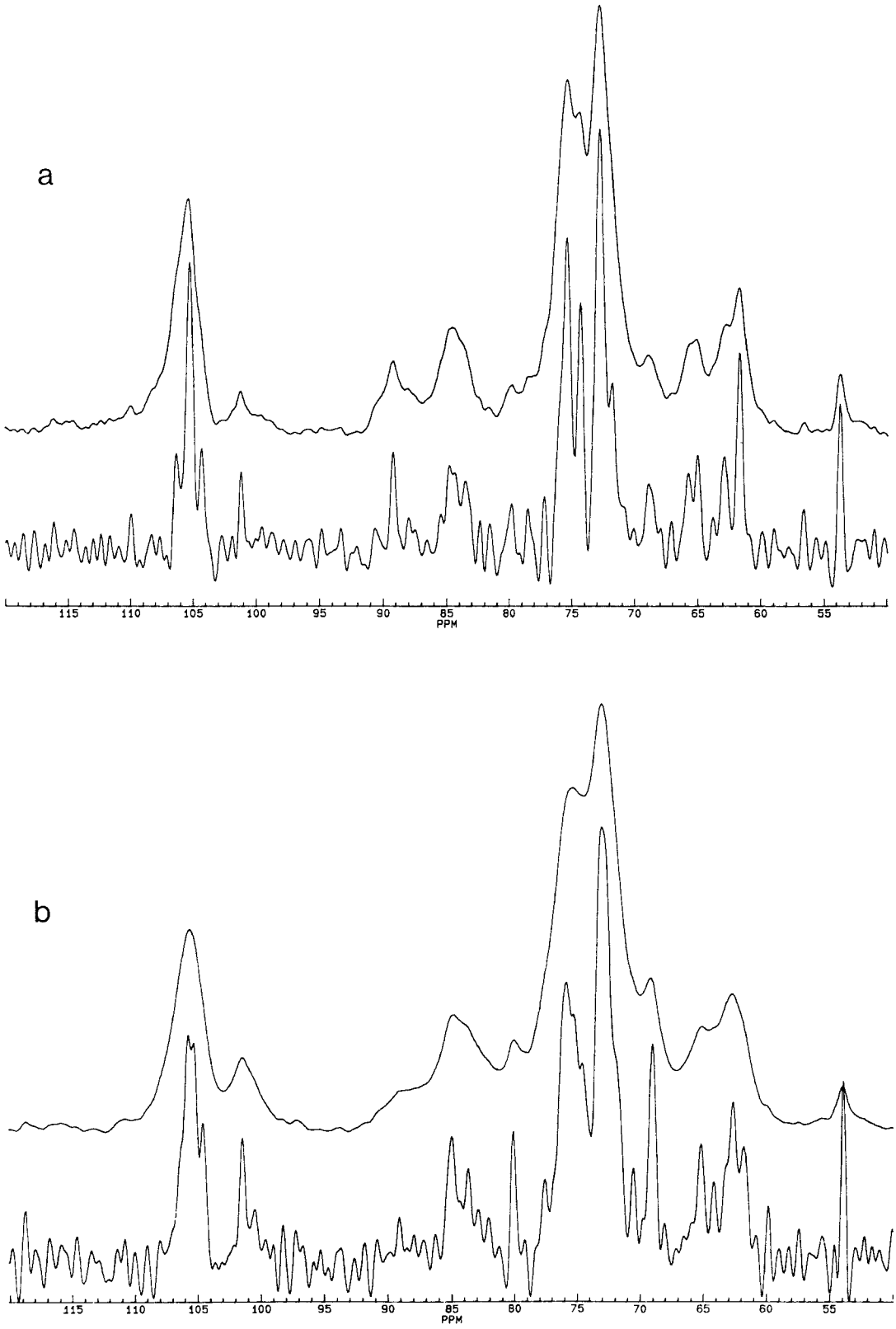

FIGURE 12 CP/DD/MAS spectra of (a) onion cell wall material (4 ms contact time) and (b) tomato cell wall material (1 ms contact time), each processed with 40 Hz line broadening (upper traces) and −70 Hz line broadening and 0.5 Gaussian multiplication (lower traces).

sis of ^{1}H $T_{1\rho}$ variation for apple cell walls. In contrast, data for dry ramie cellulose[38] clearly show relative intensity differences as a function of contact time corresponding to longer build up (T_{CH}) and decay (^{1}H $T_{1\rho}$) times for the crystalline component, therefore suggesting that spin diffusion does not average responses between crystalline and non-crystalline sites. Whether this difference is due to the cellulose source or the state of hydration remains to be determined.

We thank Lodovico Tamagnone, Sarah Whitney, Rainer Hoffmann, and Grant Reid for provision of tobacco leaf, pea stem, and red tomato pericarp cell wall materials and lupin galactan, respectively; Arthur Darke for $^1HT_2$ measurements and Karen Smith and Gill Pattullo for word processing; and the Department of Trade and Industry Agro-Food Quality LINK program for partial support of this work.

REFERENCES

1. McCann, M. C. & Roberts, K. (1991) in *The Cytoskeletal Basis of Plant Growth and Form,* Academic Press, London, Lloyd C. W., Ed., pp. 109–129.
2. Carpita, N. C. & Gibeaut, D. M. (1993) *Plant J.* **3,** 1–30.
3. Morris, E. R., Powell, D. A., Gidley, M. J. & Rees, D. A. (1982) *J. Mol. Biol.* **155,** 507–516.
4. Iiyama, K., Lam, T. B.-T. & Stone, B. A. (1994) *Plant Physiol.* **104,** 315–320.
5. Redgwell, R. J. & Selvendran, R. R. (1986) *Carbohydr. Res.* **157,** 183–199.
6. McCann, M. C., Wells, B. & Roberts, K. (1990) *J. Cell Sci.* **96,** 323–334.
7. McCann, M. C., Hammouri, M., Wilson, R., Belton, P. & Roberts, K. (1992) *Plant Physiol.* **100,** 1940–1947.
8. York, W. S., van Halbeek, H., Darvill, A. G. & Albersheim, P. (1990) *Carbohdr. Res.* **200,** 9–31.
9. Levy, S., York, W. S., Stuike-Prill, R., Meyer, B. & Staehelin, L. A. (1991) *Plant J.* **1,** 192–215.
10. Ryden, P., Colquhon, I. J. & Selvendran, R. R. (1989) *Carbohydr. Res.* **185,** 233–237.
11. Cros, S., Hervé du Penhoat, C., Bouchemal, N., Ohassan, H., Imberty, A. & Perez, S. (1992) *Int. J. Biol. Macromol.* **14,** 313–320.
12. Jarvis, M. C. & Apperley, D. C. (1990) *Plant Physiol.* **92,** 61–65.
13. Jarvis, M. C. (1990) *Carbohydr. Res.* **201,** 327–333.
14. Atalla, R. H. & VanderHart, D. L. (1984) *Science* **223,** 283–285.
15. MacKay, A. L., Wallace, J. C., Sasaki, K. & Taylor, I. E. P. (1988) *Biochemistry* **27,** 1467–1473.
16. Taylor, I. E. P., Wallace, J. C., MacKay, A. L. & Volke, F. (1990) *Plant Physiol.* **94,** 174–178.
17. Wallace, J. C., MacKay, A. L., Sasaki, K. & Taylor, I. E. P. (1993) *Planta* **190,** 227–230.
18. Irwin, P. L., Sevilla, M. D., Chamulitrat, W., Hoffman, A. E. & Klein, J. (1992) *J. Agricul. Food Chem.* **40,** 2045–2051.
19. Gidley, M. J. (1992) *Trends Food Sci. Technol.* **3:** 231–236.
20. Sutherland, J. W. H., Egan, W., Schechter, A. N. & Torchia, D. A. (1979) *Biochemistry* **18,** 1797–1803.
21. Morgan, C. F., Schleich, T., Caines, G. H. & Farnsworth, P. N. (1989) *Biochemistry* **28,** 5065–5074.
22. Garbow, J. R. & Schaefer, J. (1991) *J. Agricul. Food. Chem.* **39,** 877–880.
23. Garbow, J. R., Ferrantello, L. M. & Stark, R. E. (1989) *Plant Physiol.* **90,** 783–787.
24. Seymour, G. B., Colquhon, I. J., DuPont, S. M., Parsley, K. R. & Selvendran, R. R. (1990) *Phyotochemistry* **29,** 725–731.
25. Snape, C. E., Axelson, D. E., Botto, R. E., Delpuech, J. J., Tekely, P., Gerstein, B. C., Pruski, M., Maciel, G. E. & Wilson, M. A. (1989) *Fuel* **68,** 547–560.
26. Bloembergen, N., Purcell, E. M. & Pound, R. V. (1948) *Phys. Rev.* **73,** 679–712.
27. Harris, R. K. (1983) *Nuclear Magnetic Resonance Spectroscopy: A Physicochemical View,* Pitman, London.
28. Gidley, M. J., McArthur, A. J., Darke, A. H. & Ablett, S. (1995) in *New Physico-Chemical Techniques for the Characterisation of Complex Food Systems,* Dickinson, E., Ed., Blackie Academic, London, pp. 296–318.
29. Haw, J. F. & Johnson, N. A. (1986) *Anal. Chem.* **58,** 3254–3256.
30. Gidley, M. J. & Bociek, S. M. (1988) *Carbohydr. Res.* **183,** 126–130.
31. Ablett, S., Clark, A. H. & Rees, D. A. (1982) *Macromolecules* **15,** 597–602.
32. Yoshimizu, H., Mimura, H. & Ando, I. (1991) *Macromolecules* **24,** 862–866.
33. Yu, Y. & Brown, G. R. (1993) *Macromolecules* **26,** 4872–4877.
34. Talbott, L. D. & Ray, P. W. (1992) *Plant Physiol.* **98,** 357–368.
35. Schols, H. A. & Voragen, A. G. J. (1994) *Carbohydr. Res.* **256,** 83–95.
36. Krainer, E., Stark, R. E., Naider, F., Alagramam, K. & Becker, J. M. (1994) *Biopolymers* **34,** 1627–1635.
37. Alemany, L. B., Grant, D. M., Alger, T. D. & Pugmire, R. J. (1983) *J. Am. Chem. Soc.* **105,** 2133–2141.
38. Horii, F., Hirai, A. & Kitamaru, R. (1984) *J. Carbohydr. Chem.* **3,** 641–662.
39. Torchia, D. A. (1978) *J. Magn. Reson.* **30,** 613–616.
40. Gidley, M. J., Lillford, P. J., Rowlands, D. W., Lang, P., Dentini, M., Crescenzi, V., Edwards, M., Fa-

nutti, C. & Reid, J. S. G. (1991) *Carbohydr. Res.* **214,** 299–314.
41. Gidley, M. J., McArthur, A. J. & Underwood, D. R. (1991) *Food Hydrocoll.* **5,** 129–140.
42. Burton, B. A. & Brant, D. A. (1983) *Biopolymers* **22,** 1769–1792.
43. Renard, C. M. G. C. & Thibault, J.-F. (1993) *Carbohydr. Res.* **244,** 99–114.
44. McCann, M. C., Roberts, K., Wilson, R. H., Gidley, M. J., Gibeaut, D. M., Kim, J.-B. & Carpita, N. C. (1995) *Can. J. Bot.* **7** (suppl.), 103–113.
45. Debzi, E. M., Chanzy, H., Sugiyama, J., Tekely, P. & Excoffier, G. (1991) *Macromolecules* **24,** 6816–6822.
46. Yamamoto, H. & Horii, F. (1993) *Macromolecules* **26,** 1313–1317.
47. Newman, R. H., Ha, M.-A. & Melton, L. D. (1994) *J. Agricul. Food Chem.* **42,** 1402–1406.
48. Klemen-Leyer, K. M., Gilkes, N. R., Miller, R. C. & Kirk, T. K. (1994) *Biochem. J.* **302,** 463–469.
49. Heyraud, A., Rinaudo, M., Vignon, M. & Vincendon, M. (1979) *Biopolymers* **18,** 167–185.